Design, Synthesis and Anticancer Activity Evaluation of Novel Quinazoline Derivatives as EFGR Inhibitors①

LI Hong-Xia② QIAN Yu-Mei XU Li-Sheng

(*School of Life and Food Engineering, Suzhou University, Suzhou* 234000, *China*)

ABSTRACT Malignant tumor is one of the major diseases that seriously threaten human health today. Compared with traditional chemotherapy, targeted drug therapy has become a new idea of tumor therapy. And EGFR (epidermal growth factor receptor) is highly expressed in many human tumor cell lines, which is a biomarker of tumor proliferation. In this paper, small molecule tyrosine kinase inhibitors with quinazoline structure aiming at EGFR were studied. A series of novel quinazoline derivatives (**4a~4l**) have been designed and synthesized from 4-hydroxyquinazoline as the parent core. Structures of target compounds were characterized by ^{1}H NMR and ^{13}C NMR spectra. The *in vitro* anticancer activity of compounds **4a~4l** was evaluated by MTT assay against Hela, MCF-7 and A549 tumor cell lines, and apoptosis-inducing capacity was investigated by Annexin-V/PI staining assay. The results showed that all compounds had good antitumor activity against the test tumor cell lines. Especially, compound **4a** exhibited the best anticancer activity (IC_{50} = 10.23 μM) against Hela cell lines, remarkable ability to induce apoptosis, and low toxicity, which identified **4a** as a promising anticancer drug aiming at EFGR.

Keywords: **hydroxyquinazoline, EFGR, antitumor activity, toxicity, apoptosis;**

DOI: 10.14102/j.cnki.0254–5861.2011–3082

1 INTRODUCTION

Cancer, as a second-leading disease of death worldwide, has been seriously threating people's health[1]. Most cancers are due to a series of complex causes including people's problematic lifestyle, diet and the environment they live in; however, among them, the genetic mutations are believed as the most complex and uncontrollable factor[2]. At the moment, cancer is often treated with radiation therapy, chemotherapy, and immunotherapy[3]. These treatments can to some extent kill tumor cells; however, such methods are non-specific without the ability to distinguish tumors from normal tissues, then many toxic and side effects can be therefore anticipated because the growth and the activity of normal cells are adversely affected. In addition, it is also claimed that all these mentioned therapies are expensive and more likely to develop drug resistance.

Amid this background, targeted therapy, driven by the progress of molecular biology and tumor pathogenesis, has emerged and made a vast difference in today's cancer treatment[4]. This method can specially interfere with the proliferation of tumor cells by using some compounds like small molecular compounds, monoclonal antibodies and polypeptides which target at cell receptors, regulatory molecules or key genes before inhibiting the development of malignant tumors. These compounds, after entering patients' body, can bind to their designed targets specifically, thus causing specific death of specific tumor cells and leaving other cells being unaffected[5]. In order to better achieve this purpose, a new challenge that how to develop the upgraded anti-tumor drugs with high efficiency, low toxicity and strong specificity and how to choose some key proteins in the signal transduction pathway of tumor cell proliferation and differentiation has become both tough and exciting recently.

In this process, Tyrosine Protein Kinase (TPK), as one of the effective potential target spots, has been studied in a wide aspect[6]. It is an important protein that controls both the growth and the differentiation of cells[7]; it also plays a key role in normal cell division and abnormal cell proliferation[8]. TPK includes three types and one is Receptor Tyrosine

Received 28 December 2020; accepted 12 March 2021

① This work was financially supported by the Suzhou University Natural Science Key Project (No. 2017yzd11, 2020ykf23, 2020ykf24), National Engineering Laboratory Open Fund Project (NEL-SCRT 002), and Natural Science Foundation of An Hui Province (No. 1908085MC100，KJ2020A0729, KJ2020A0737)

② Corresponding author. E-mail: szxy2016hx@163.com

Kinase (RTK). Meanwhile, as a type of RTK, Epidermal Growth Factor Receptor (EGFR) has been studied as an essential target spot for the targeted therapy of epidermal tumors, aiming to develop some novel EFGR-TPK inhibitors[9]. EGFR mediates intracellular signal transduction and regulates cell proliferation and differentiation. It is reported that 30% to 50% of epidermal tumors which include cervical cancer, breast cancer, esophageal cancer, etc. in humans show overexpression or abnormal mutations[10]. It may lead to more developed signal transduction of cells, causing the formation and the development of malignant tumors.

At the moment, two main EGFR inhibitors, quinazolines and pyrimidines, have been studied[11]. Quinazoline is a kind of natural alkaloid and its derivatives show many biological characteristics, such as hypnosis[11], analgesia[12] and anti-inflammatory[13]. These derivatives, which have the proved function of anti-cancer[14], anti-bacteriostatic, anti-virus, etc., are a recent focus of the research on tumor drugs. Several anti-cancer drugs using EGFR as their target spot and also containing such derivative structure have been marketed, representing the first and second generation EFGR inhibitors[15]. The first-generation EGFR inhibitors include Gefitinib, Erlotinib, Lapatinib, and so on[16]. These reversible inhibitors can effectively interrupt the downstream signal transduction of EGFR expression pathway; however, the emerging drug resistance, particularly caused by the T790M mutation, compromises its efficacy. For better solving this problem, the second generation of irreversible inhibitors, such as Neratinib, Dacomitinib, Afatinib and so forth were developed[17]. Afatinib, as the first irreversible model of the second generation of EFGR inhibitor approved by the US Food and Drug Administration (FDA), has achieved to the Phase III in pancreatic cancer, thyroid cancer and metastatic renal cell carcinoma[18]. However, it has serious side effects, such as skin rash and gastrointestinal toxicity. The third generation of pyrimidine EFGR inhibitor therefore came out in this background[19]. AZD9291 and Rocictinib, for example, can partly reduce drug resistance and side effects; however, since its potential side effects still exist, it calls for continuous efforts. Many teams have synthesized and studied 4-sustituted quinazoline derivatives to understand their abilities in anti-tumor[20], anti-inflammation[21] and anti-virus[22, 23]. Given the conducted researches, an experiment, using 4-hydroxyquinazoline as the parent core and taking a three-step reaction to create 12 novel quinazoline derivatives, was designed. By evaluating the antitumor ability of the derivatives and analyzing the relations between the ability and structures, the experiment below will serve as a possible academic basis for future study on cancer drugs featured by quinazoline derivatives.

2 EXPERIMENTAL

2. 1 Chemistry

Quinazoline derivatives **4a~4l** were synthesized as outlined in Scheme 1. 4-Hydroxyquinazoline was treated with ethyl bromoacetate to offer intermediate **2**, which was then treated with hydrazine hydrate to give intermediate **3**. **3** separately reacts with different aldehydes to obtain target compounds **4a~4l**. The structures of quinazoline derivatives (Table 1) were confirmed by ^{1}H NMR and ^{13}C NMR spectra.

Table 1. Structures of Compounds 4a~4l

Compounds	n	R^1	R^2	R^3
4a	0	H	H	OCH_3
4b	0	Cl	H	H
4c	0	H	Cl	H
4d	0	H	H	Cl
4e	0	H	Br	H
4f	0	H	H	Br
4g	1	H	H	H
4h	0	OH	H	H
4i	0	H	H	OH
4j	0	H	H	NO_2
4k	0	H	H	H
4l	0	F	H	H

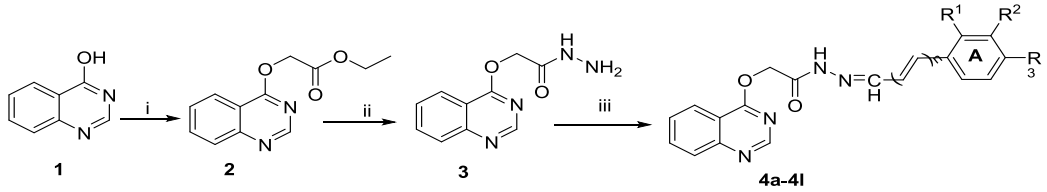

Scheme 1: Reagents and conditions: (i) Ethyl bromoacetate, acetone, 50 ℃, 10 h; (ii) Hydrazine hydrate, ethanol, 80 ℃, 5 h; (iii) Ethanol, aromatic aldehydes, r.t., 2~3 h

4-Hydroxyquinazoline (1 mmol) dissolved in acetone was heated to reflux for 10 h with ethyl bromoacetate (1 mmol). After reaction, the mixture was filtered and extracted with ethyl acetate, and the solvent was evaporated under reduced pressure to offer intermediate **2**. After recrystallization, the pure intermediate **2** and hydrazine hydrate were added to anhydrous ethanol and the mixture was refluxed at 80 ℃ for 5 h. The sample was monitored by TLC. The mixture was poured into ice water mixture (50 mL). After the material was precipitated, pure intermediate **3** was given by recrystallization with anhydrous ethanol. Intermediate **3** added to anhydrous ethanol was separately reacted with different aldehydes and a few drops of glacial acetic acid, and the mixture was stirred for another 2~3 hours until TLC indicated the complete reaction. The solution was concentrated at reduced pressure and the crude product was purified by chromatography on silica gel or recrystallization with anhydrous ethanol to offer compounds **4a~4l**.

2. 2 *In vitro* antitumor activity related to the structure

The *in vitro* antitumor activities of test compounds **4a~4l** were evaluated by MTT assay against Hela, MCF-7 and A549 tumor cell lines at concentrations of 10, 20, 50 and 100 μM. The tested results are shown in Table 2, in which most compounds exhibited inhibitory activity, and had better activity against Hela and MCF-7 cells than A549 cells. Among the 12 compounds, **4a** showed the best cytotoxicity activity with the IC_{50} values to be 10.23, 12.78 and 15.12 μM, close to the value of the positive control drug Gefitinib (8.84, 7.12, 9.44 μM).

Table 2. *In vitro* Antitumor Activities of Compounds 4a~4l against MCF-7, Hela, A549 Cell Lines

Compounds	IC_{50} ± SD (μM) [b]		
	MCF-7	Hela	A549
4a	12.78 ± 1.78	10.23 ± 1.34	15.12 ± 1.23
4b	30.45 ± 1.66	27.02 ± 0.78	33.87 ± 0.87
4c	24.32 ± 1.80	23.10 ± 1.50	30.7 ± 0.94
4d	18.94 ± 1.79	21.92 ± 1.25	28.12 ± 1.01
4e	28.08 ± 0.63	20.68 ± 0.74	36.54 ± 1.35
4f	22.98 ± 0.94	15.31 ± 1.48	27.13 ± 1.25
4g	31.97 ± 0.26	33.08 ± 1.04	>50
4h	24.48 ± 0.70	30.37 ± 0.67	38.35 ± 0.48
4i	27.95 ± 1.06	26.22 ± 1.30	37.12 ± 1.65
4j	21.34 ± 1.26	24.46 ± 1.54	33.76 ± 0.51
4k	35.78 ± 1.08	30.23 ± 1.27	>50
4l	23.78 ± 1.56	25.89 ± 0.87	28.86 ± 0.35
Gefitinib[a]	8.84 ± 0.19	7.12 ± 0.43	9.44 ± 2.35

[a] Used as a positive control; [b] The IC_{50} values represent an average of three experiments ± SD.

The data indicate that differences in the positions of the same substituent or the substituents at the same position cause differences in antitumor activity. Taking MCF-7 cells as an example, compounds **4b**, **4c**, and **4d** were all replaced by chloride ions. The antitumor activity of para-substituted compound **4d** (IC_{50} = 18.94 μM) was better than that of

meta-substituted compound **4c** (IC_{50} = 24.32 μM), while **4c** was also superior to ortho-substituted compound **4b** (IC_{50} = 30.45 μM). After being substituted by the same halogen atom at different positions, the antitumor activity sequence is para > meta > ortho.

Compound **41** (IC_{50} = 23.78 μM), which was replaced by a fluoride ion in the ortho position, was superior to compound **4b** (IC_{50} = 30.45 μM) in which the ortho position was replaced by a chloride ion. And compound **4c** (IC50 = 24.32 μM) replaced by chloride ion in the meta position was better **4e** (IC_{50} = 28.08 μM) where the same position was replaced by a bromide ion. When the same position is substituted by a different halogen atom, the antitumor activity sequence is a fluorine atom > a chlorine atom > a bromine atom.

The meta positions of compounds **4a**, **4i**, and **4j** were substituted by methoxy, nitro and hydroxy. **4a** (IC_{50} = 12.78 μM) preceded **4j** (IC_{50} = 21.34 μM)), which was better than the **4i** (IC_{50} = 27.95 μM). After the compound is substituted by a different group, the order of activity is methoxy > nitro > hydroxy.

Compounds **4g** (IC_{50} = 31.97 μM) and **4k** (IC_{50} = 35.78 μM) without a substituent had low antitumor activity. The data of the other two cells also have the same conclusion.

2. 3 *In vitro* EGFR inhibitory activities

All target compounds (**4a~4l**) were evaluated for their inhibitory activities on EGFR using solid-phase ELISA kit, with **Erlotinib** as the positive control drug. The results are summarized in Table 3, which suggested that majority of the tested compounds exhibited sufficiently potent anti-cancer activity. Among them, although compound **4a** displayed the most significant EGFR inhibitory activity with IC_{50} value of 2.8 μM, weak to the reference EGFR selective inhibitor **Erlotinib** (IC_{50} = 1.42 μM).

The following structure-activity relationship (SAR) studies were performed to determine how the substituents affect the EGFR inhibitory activity. When substituents R^1 and R^2 remained unchanged, selection of different substituents R^3 against EGFR indicated strong electron-donating groups are preferable than the electron-withdrawing groups, comparing compound **4a** (IC_{50} = 2.80 μM) = **4i** (IC_{50} = 2.80 μM) > **4d** (IC_{50} = 4.3 μM) > **4f** (IC_{50} = 5.6 μM) > **4j** (IC_{50} = 42 μM). Similarly, when the *ortho*-position of A ring was substituted by electron-donating group, the EGFR inhibitory activity was also better than the electron-withdrawing groups. The above analysis suggested that electron-donating groups substituted on the *para*-position or *ortho*-position of A ring play a crucial role in the inhibitory activity.

Table 3. Inhibition Activities of Compounds 4a~4l against EGFR

Compounds	Compounds	IC_{50} (μM)[a]		
	EGFR[b]		EGFR[b]
4a	2.8	**4h**	4.6
4b	6.3	**4i**	2.8
4c	18.1	**4j**	42
4d	5.6	**4k**	3.2
4e	8.9	**4l**	10.2
4f	4.3	**Erlotinib**	1.42
4g	9.6		

[a] Errors were in the range of 5~10% of the reported values, from three different assays.

[b] Human recombinant enzymes, by the esterase assay (4-nitrophenylacetate as substrate).

2. 4 Compound 4a inducing apoptosis in the Hela cells

Compound **4a** with the best antitumor activity was selected for apoptosis study against Hela cells, which was analyzed by flow cytometry after staining with Annexin V-FITC and PI. The experimental groups of drug concentration gradient were designed. Fig. 1 shows that **4a** can induce apoptosis in Hela cells. There were fewer apoptotic and dead cells in the blank group without drug and the normal cells grew well. A dose-dependent increase in the percentage of apoptotic cells was evaluated after the cells were treated with compound **4a** for 24 h at different concentrations of 2, 4 and 8 μM. The proportion of death was 17.15%, 25.5% and 34.6% along with the concentration gradient. The results confirmed that compound **4a** could effectively induce apoptosis in Hela cells, indicating its good apoptosis-inducing activity.

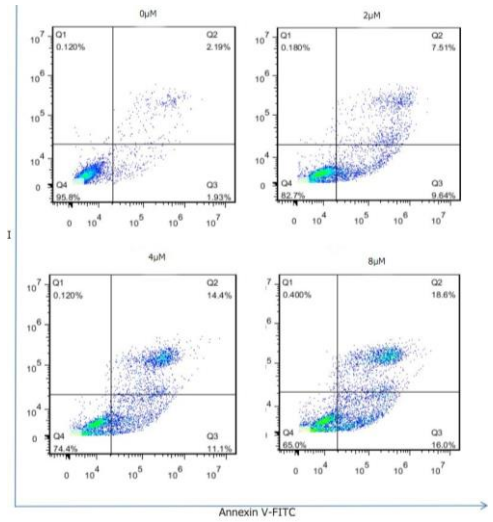

Fig. 1. Apoptosis rate of Hela cells treated with 4a (0, 2, 4 and 8 μM) for 24 h

2. 5 Compounds 4a~4l with low cytotoxicity

The cytotoxicity study was carried out for further information about the biosecurity. Gefitinib was used as a positive control. As shown in Table 4, these compounds had little cytotoxicity similar to or lower than the positive control drug and were potentially antitumor drugs with low toxicity.

Table 4. Cytotoxicity Assay by Compounds 4a~4l

Compounds	CC_{50} ± SD (μM) 293T	Compounds	CC_{50} ± SD (μM)[c] 293T
4a	243.05 ± 1.23	**4h**	225.43 ± 1.44
4b	198.46 ± 0.43	**4i**	207.54 ± 1.85
4c	213..13 ± 1.86	**4j**	223.77 ± 3.27
4d	215.58 ± 1.78	**4k**	213.75 ± 1.89
4e	234.26 ± 1.87	**4l**	218.07 ± 2.64
4f	216.14 ± 1.27	**Gefitinib**	231.23 ± 1.56
4g	186.47 ± 1.67		

[c] The averaged values determined by three separate determinations.

3 RESULTS AND DISCUSSION

3. 1 Materials and measurements

All chemical agents were analytically pure and used without further purifications. All of them were available on market and purchased from Aladdin or Sinopharm without special instructions. The solution was concentrated at reduced pressure by a rotary evaporator (Chang cheng, Zhengzhou). Bruker's DPX600 NMR spectrometer was used to get ^{1}H NMR and ^{13}C NMR spectra. Chemical shifts were expressed in ppm (TMS as internal standard) and coupling constants (*J*) in Hz. Melting points were measured using Tektronix Melting Point Instrument-XT4. All cell experiments were operated in a BCN-1360 ultra clean bench, and cells were incubated in a Heracel CO_2 incubator. The light absorption (OD value) was measured by a microplate reader (TECAN, Austria). Flow cytometry studies were carried out by a FACSAria III flow cytometer (BD).

3. 2 General procedure for the synthesis of compound 2

Compound 4-hydroxyquinazoline (2 mmol), ethyl bromoacetate (2 mmol) and acetone (10 mL) were added to a 25 mL round bottom flask under stirring and the reaction was stirred at 50 ℃ for 10 h, and then poured onto distilled water. The reaction mixture was extracted with ethyl acetate (100 mL × 3) and water (100 mL × 3) and dried under vacuum. The resulting solid was dissolved in absolute ethanol to give crystalline intermediate **2**.

3. 3 General procedure for the synthesis of compound 3

Intermediate **2** (1 mmol), absolute ethanol (15 mL) and hydrazine hydrate (1 mL) were added to a 25 mL round

bottom flask under stirring and the reaction was stirred at 80 ℃ for 5 h, and then poured into water and filtered. The solid was washed with distilled water (3 × 50 mL) and dried under vacuum. The resulting solid was dissolved in absolute ethanol to give crystalline intermediate **3**.

3. 4 General procedure for the syntheses of compounds 4a~4l

A solution of intermediate **2** (0.8 mmol) and aromatic aldehydes (0.8 mmol) in absolute ethanol (10 mL) was stirred at room temperature for 3 h. The reaction mixture was concentrated under reduced pressure. The crude product was purified by silica gel column chromatography (V_{EtOAc}/V_{PE} = 1:1) to give compounds **4a**~**4l**.

3. 4. 1 (*E*)-*N*′-(4-methoxybenzylidene)-2-(quinazolin-4-yloxy)acetohydrazide (4a)

White solid, 0.153 g, yield: 57%, melting point: 126.8~127.7 ℃. ^{1}H NMR (DMSO-d_6, 600 MHz) δ 11.23 (s, 1H), 11.12 (s, 1H), 8.08 (s, 1H), 7.92 (s, 1H), 7.58~7.62 (m, 2H), 6.98~7 (m, 3H), 3.79 (s, 3H), 3.34 (s, 1H), 2.17 (s, 2H), 1.93 (s, 1H); ^{13}C NMR(151 MHz, $CDCl_3$) δ 176.92, 170.53, 165.87, 165.68, 150.72, 150.59, 147.63, 147.52, 133.73, 133.37, 132.11, 119.51, 119.45, 60.48, 60.47, 45.14, 44.86, 44.30, TOF MS EI$^+$ *m*/*z*: 336.3.

3. 4. 2 (*E*)-*N*′-(2-chlorobenzylidene)-2-(quinazolin-4-yloxy)acetohydrazide (4b)

White solid, 0.183 g, yield: 67%, melting point: 135.3~135.7 ℃. ^{1}H NMR (DMSO-d_6, 600 MHz) δ 11.61 (s, 1H), 11.45 (s, 1H), 8.53 (s, 1H), 8.38 (s, 1H), 7.93~7.99 (m, 1H), 7.50~7.52 (m, 1H), 7.40~7.43 (m, 3H), 3.34 (s, 1H), 2.22 (s, 2H), 1.97 (s, 1H); ^{13}C NMR(151 MHz, $CDCl_3$) δ 177.34, 170.96, 146.66, 143.75, 143.71, 138.20, 136.75, 136.24, 135.09, 132.77, 131.94, 131.73, 45.15, 44.73, 44.45, 26.88, 25.48, TOF MS EI$^+$ *m*/*z*: 340.8.

3. 4. 3 (*E*)-*N*′-(3-chlorobenzylidene)-2-quinazolin-4-yloxy)acetohydrazide (4c)

White solid, 0.190 g, yield: 70%, melting point: 165.9~166.5 ℃. ^{1}H NMR (DMSO-d_6, 600 MHz) δ 11.44 (s, 1H), 11.31 (s, 1H), 8.07 (s, 1H), 7.90 (s, 1H), 7.66~7.68 (d, *J* = 11.4Hz, 1H), 7.55~7.59 (m, 1H), 7.39~7.41 (m, 3H), 3.28 (s, 1H), 2.15 (s, 2H), 1.90 (s, 1H); ^{13}C NMR(151 MHz, $CDCl_3$) δ 177.35, 171.00, 149.14, 146.12, 141.86, 138.35, 135.88, 134.67, 131.43, 131.20, 130.65, 45.00, 44.73, 44.87, 44.45, 26.85, 25.49, TOF MS EI$^+$ *m*/*z*: 340.8.

3. 4. 4 (*E*)-*N*′-(3-chlorobenzylidene)-2-(quinazolin-4-yloxy)acetohydrazide (4d)

White solid, 0.196 g, yield: 72%, melting point: 146.5~147.2 ℃. ^{1}H NMR (DMSO-d_6, 600 MHz) δ 11.43 (s, 1H), 11.31 (s, 1H), 8.13 (s, 1H), 7.97 (s, 1H), 7.67~7.71 (m, 2H), 7.48~7.50 (m, 2H), 3.34 (s, 2H), 2.20 (s, 2H), 1.95 (s, 1H); ^{13}C NMR(151 MHz, $CDCl_3$) δ 177.23, 170.87, 149.51, 146.45, 139.48, 139.25, 138.55, 138.46, 134.08, 133.78, 133.47, 45.01, 44.87, 44.73, 44.45, 26.86, 25.45, TOF MS EI$^+$ *m*/*z*: 340.8.

3. 4. 5 (*E*)-*N*′-(3-bromobenzylidene)-2-(quinazolin-4-yloxy)acetohydrazide (4e)

White solid, 0.188 g, yield: 61%, melting point: 163.9~165.4 ℃. ^{1}H NMR (DMSO-d_6, 600 MHz) δ 11.50 (s, 1H), 11.36 (s, 1H), 8.11 (s, 1H), 7.95 (s, 1H), 7.88 (s, 1H), 7.85 (s, 1H), 7.65~7.68 (m, 1H), 7.58~7.60 (m, 1H), 7.37~7.41 (m, 1H), 3.34 (s, 1H), 2.20 (s, 2H), 1.96 (s, 1H); ^{13}C NMR(151 MHz, $CDCl_3$) δ: 177.34, 171.00, 149.03, 148.89, 146.04, 145.92, 142.09, 137.56, 136.19, 134.32, 133.97, 131.23, 127.32, 45.01, 44.73, 26.85, 25.51, TOF MS EI$^+$ *m*/*z*: 385.2.

3. 4. 6 (*E*)-*N*′-(4-bromobenzylidene)-2-(quinazolin-4-yloxy)acetohydrazide (4f)

White solid, 0.188 g, yield: 61%, melting point: 51.8~152.6 ℃. ^{1}H NMR (DMSO-d_6, 600 MHz) δ 11.44 (s, 1H), 11.32 (s, 1H), 8.12 (s, 1H), 7.95 (s, 1H), 7.63 (s, 2H), 7.61-7.62 (d, *J* = 2.52Hz, 3H), 3.34 (s, 1H), 2.20 (s, 2H), 1.95 (s, 1H); ^{13}C NMR(151 MHz, $CDCl_3$) δ 177.24, 170.88, 149.59, 146.55, 146.44, 138.89, 136.98, 134.02, 133.71, 128.25, 128.00, 45.01, 44.87, 44.59, 44.45, 26.86, 25.45, TOF MS EI$^+$ *m*/*z*: 385.2.

3. 4. 7 *N*′-((1*E*,2*E*)-3-phenylallylidene)-2-(quinazolin-4-yloxy)acetohydrazide (4g)

Yellow solid, 0.194 g, yield: 73%, melting point: 159.5~160.7 ℃. ^{1}H NMR (DMSO-d_6, 600 MHz) δ 11.15 (s, 1H), 7.80~7.81 (d, *J* = 7.86Hz, 1H), 7.58~7.60 (d, *J* = 7.32Hz, 3H), 7.36~7.39 (m, 3H), 6.94~7.00 (m, 2H), 3.35 (s, 1H), 2.12 (s, 3H), 1.92 (s, 2H); ^{13}C NMR(151 MHz, $CDCl_3$) δ 172.15, 165.9, 148.00, 145.59, 138.95, 138.63, 136.40, 129.29, 129.20, 129.14, 127.45, 126.10, 125.74, 40.26, 40.12, 39.98, 39.70, 22.08, 20.72, TOF MS EI$^+$ *m*/*z*: 332.4.

3. 4. 8 (*E*)-*N*′-(2-hydroxybenzylidene)-2-(quinazolin-4-yloxy)acetohydrazide (4h)

White solid, 0.172 g, yield: 67%, melting point: 193.5~195.2 ℃. ^{1}H NMR (DMSO-d_6, 600 MHz) δ 11.19 (s, 1H), 8.33 (s, 1H), 8.26 (s, 1H), 8.33 (s, 1H), 7.49~7.50 (d, *J* = 8.82Hz, 1H), 7.22~7.29 (m, 1H), 6.85-6.91 (m, 3H), 3.33 (s, 1H), 2.18 (s, 2H), 1.97 (s, 2H); ^{13}C NMR(151 MHz, $CDCl_3$) δ 176.72, 170.62, 162.51, 161.56, 151.42, 146.10, 145.97,

136.41, 134.63, 131.96, 125.21, 124.50, 123.80, 121.56, 44.99, 26.58, 25.56, TOF MS EI$^+$ *m*/*z*: 322.3.

3. 4. 9 (*E*)-*N*′-(4-hydroxybenzylidene)-2-(quinazolin-4-yloxy)acetohydrazide (4i)

Yellow solid, 0.154 g, yield: 69%, melting point: 238.3~239.9 ℃. ^{1}H NMR (DMSO-d_6, 600 MHz) δ 11.04 (s, 1H), 9.85 (s, 1H), 7.88 (s, 1H), 7.47~7.50 (m, 3H), 6.80~6.82(m, 3H), 3.35 (s, 1H), 2.16 (s, 3H), 1.91 (s, 1H); ^{13}C NMR (151 MHz, $CDCl_3$) δ 172.06, 165.68, 159.67, 159.47, 146.35, 143.26, 129.14, 128.76, 125.77, 116.11, 116.08, 40.24, 39.96, 39.82, 39.68, 22.07, 20.70. TOF MS EI$^+$ *m*/*z*: 322.3.

3. 4. 10 (*E*)-*N*′-(4-nitrobenzylidene)-2-(quinazolin-4-yloxy)acetohydrazide (4j)

Yellow solid, 0.160 g, yield: 57%, melting point: 173.8~174.9 ℃. ^{1}H NMR (DMSO-d_6, 600 MHz) δ 11.68 (s, 1H), 11.56 (s, 1H), 8.25~8.29 (m, 3H), 8.08 (s, 1H), 7.91~7.95 (m, 3H), 3.34 (s, 1H), 2.24 (s, 2H), 2.0 (s, 1H); ^{13}C NMR (151 MHz, $CDCl_3$) δ 172.83, 166.49, 148.16, 147.99, 143.54, 141.23, 141.09, 140.59, 128.30, 127.98, 124.48, 40.25, 39.97, 39.83, 39.69, 22.15, 20.69, TOF MS EI$^+$ *m*/*z*: 351.32.

3.4. 11 (*E*)-*N*′-benzylidene-2-(quinazolin-4-yloxy)acetohydrazide (4k)

White solid, 0.186 g, yield: 57%, melting point: 133.4~134.9 ℃. ^{1}H NMR (DMSO-d_6, 600 MHz) δ 11.37 (s, 1H), 11.25 (S, 1H), 8.14 (S, 1H), 7.98 (S, 1H), 7.65~7.68 (m, 2H), 7.40~7.44 (m, 4H), 3.33 (S, 1H), 2.20 (S, 2H), 1.95 (S, 1H); ^{13}C NMR (100 MHz, $CDCl_3$) δ 177.17, 170.80, 150.83, 150.70, 147.75, 147.63, 139.58, 139.51, 134.86, 134.00, 132.16, 131.84, 45.00, 44.73, 44.45, 26.86, 25.46, TOF MS EI$^+$ *m*/*z*: 408.8.

3. 4. 12 (*E*)-*N*′-(2-fluorobenzylidene)-2-(quinazolin-4-yloxy)acetohydrazide (4l)

White solid, 0.110 g, yield: 74%, melting point: 132.1~134.3 ℃. ^{1}H NMR (DMSO-d_6, 600 MHz) δ 10.56 (s, 1H), 10.42 (s, 1H), 7.47 (s, 1H), 7.24 (s, 1H), 6.93~6.90 (m, 1H), 6.51~6.4 (m, 1H), 6.33~6.29 (m, 3H), 1.55~1.54 (m, 2H), 1.25 (s, 1H), 1.00 (s, 1H). ^{13}C NMR (151 MHz, $CDCl_3$) δ 172.53, 166.14, 161.95, 161.84, 160.30, 138.73, 135.78, 131.97, 126.71, 126.52, 125.34, 122.32, 116.46, 40.09, 39.81, 22.10, 20.64, TOF MS EI$^+$ *m*/*z*: 324.3.

4 BIOLOGICAL ASSAYS

4. 1 Cell culture

A549, Hela and MCF-7 tumor cell lines were cultured in dulbecco's modified eagle medium (DMEM) containing 10% fetal calf serum (Sijiqing Technologies) and 1% antibiotics (100 units/mL penicillin and 100 mg/mL streptomycin), incubated at 37 ℃ in a 5% CO_2 incubator. Cells were collected after digestion by trypsin (Sigma) and the supernatant was discarded after centrifugation at 1100 RPM for 5 min.

4. 2 Anti-tumor activity test

The *in vitro* anti-tumor potency of test compounds **4a~4l** was evaluated by MTT assay against A549, Hela, MCF-7 tumor cell lines, with Gefitinib as the positive control.

A bottle of cells that have just grown into a complete monolayer was collected. Then two drops of cell suspension were dyed by Trypan Blue and the number of viable cells was calculated under the microscope (The number of dead cells should not exceed 5%). And the density of cells was adjusted to 1 × 10^5 cells/mL with complete medium. Cell suspension (100 μL) were seeded into each well in a 96-well plate and incubated in a CO_2 incubator for 12 hours. Then the cells in each well were treated with the sample of indicated concentrations (100 μL) for another 24 hours. The final concentration of the drug was 10, 20, 50, 100 μM, and each group was repeated in six wells. We also designed a blank group without solution, a no-dosing group with solution and cells and a positive control group treated by Gefitinib, a first-generation EFGR inhibitor. 10 μL MTT (5 mg/mL) was added to each well, and the mixture was shaken and cultured for 4 hours. The light absorption (OD value) of each well was measured by a microplate reader (TECAN, Austria) followed by three repeats, and the excitation wavelength was at 490 nm. The IC_{50} value of the drug for selected cell proliferation was calculated according to the OD value of each well.

4. 3 *In vitro* EGFR inhibition assay

The ability of the synthesized compounds to inhibit EGFR was determined by ELISA Kit. Compounds **4a~4l** were dissolved in 100% DMSO and diluted to the appropriate concentrations with 25 mM HEPES at pH 7.4. In each well, 10 μL compound was incubated with 10 μL (5 ng for EGFR) recombinant enzyme (1:80 dilution in 100 mM HEPES) for 10 min at room temperature. Then, 10 μL of 5 mM buffer (containing 20 mM HEPES, 2 mM $MnCl_2$, 100 μMNa_3VO_4, and 1 mM DTT) and 20 μL of 0.1 mM ATP-50 mM $MgCl_2$ were added for 1 h. Positive and negative controls were included in each plate by incubation of enzyme with or without ATP-$MgCl_2$. At the end of incubation, liquid was

aspirated, and plates were washed three times with wash buffer. A 75 μL (400 ng) sample of europium labeled anti-phosphotyrosine antibody was added to each well for another 1 h of incubation. After washing, enhancement solution was added and the signal was detected by Victor (Wallac Inc.) with excitation at 340 nm and emission at 615 nm. The percentage of auto-phosphorylation inhibition by the compounds was calculated using the following formula: 100%-[(negative control)/(positive control-negative control)]. The IC_{50} was obtained from curves of percentage inhibition with eight concentrations of compound. As the contaminants in the enzyme preparation are fairly low, the majority of the signal detected by the anti-phosphotyrosine antibody is from EGFR.

4. 4 Apoptosis test

In order to confirm whether **4a** was also responsible for the induction of apoptosis, Hela cells were co-stained with Annexin-V FITC and PI, and the number of apoptotic cells was estimated by flow cytometry.

Hela cells in the logarithmic phase were collected and adjusted to a concentration of 1.0×10^5 cells/mL. Cells were seeded at 6-well plates at 2 mL per well. After plates were incubated inside the CO_2 incubator at 37 ℃ for 12 hours, compound **4a** with the strongest inhibitory activity was added as the apoptosis induction drug, and the drug concentrations were 0, 2, 4, and 8 μM. Equivalent cell suspension was added to blank control. After another 24 hours, the cells were washed twice with cold Phosphate Buffered Saline (PBS) and then resuspend cells in Binding Buffer (500 μL). FITC Annexin V (5 mL) and propidium iodide (PI, 5 mL) were added to each well. Cells were gently vortexed incubated for 15 min at room temperature (25 ℃) in the dark. The cells were transferred into polypropylene tubes and analyzed by a FACSAria III flow cytometer. Data analysis and plotting were performed using Flowjo 7.6.1 (FACSCA2BUR, Becton Dickinson, USA).

4. 5 Cytotoxicity test

Cytotoxicity was assessed using human embryonic kidney epithelial cells 293T. 293T cells in the logarithmic growth phase were seeded in 96-well plates 100 μL per well at a density of 1×10^5 cells/mL. After incubation at 37 °C in a 5% CO_2 incubator, LPS was added to LPS control groups and the normal group without LPS and drug served as a blank control. In the drug group, after adding different concentrations of the test drug **4a**, LPS (final concentration was 1 mg/L) was added to stimulate the cells for 24 h, and each group was repeated in 3 wells. After incubation for 24 h, 15 μL of 5 mg/mL MTT solution was added to each well, and the plates were kept for 4 h at 37 °C in a 5% CO_2 incubator. Then liquid in the well was removed, and the crystals generated from viable cell were dissolved by DMSO (150 μL) in each well. The plates were swirled gently for 8~10 min to dissolve the precipitate, and quantified by measuring the optical density (OD) of each well at a wavelength of 570 nm using a microplate reader.

5 CONCLUSION

In summary, we have developed a series of novel quinazoline derivatives **4a~4l** that possessed relatively good inhibitory activity against the test tumor cell lines, remarkable ability to induce apoptosis, and low toxicity. Especially, compound **4a** exhibited the best anticancer activity against Hela cell lines, which suggested us the potential of **4a** as a promising anticancer drug aimed at EFGR.

REFERENCES

(1) Wang, Y. C.; Long, J. B.; Gao, H.; Tang, Z. L. 2-Aminothiazole: a privileged scaffold for the discovery of anti-cancer agents. *Eur. J. Med. Chem.* **2020**, 210, 112953–112967.

(2) Ferlay, J.; Soerjomataram, I.; Dikshit, R.; Eser, S.; Mathers, C.; Rebelo, M.; Parkin, D. M.; Forman, D.; Bray, F. Cancer incidence and mortality worldwide: sources, methods and major patterns in GLOBOCAN 2012. *Inter. J. Cancer.* **2015**, 136, E359–86.

(3) Mahoney, K. M.; Rennert, P. D.; Freeman, G. J. Combination cancer immunotherapy and new immunomodulatory targets. *Nat. Rev. Drug Discov.* **2015**, 14, 561–584.

(4) Michot, J. M.; Bigenwald, C.; Champiat, S.; Collins, M.; Carbonnel, F.; Postel-Vinay, S.; Berdelou, A.; Varga, A.; Bahleda, R.; Hollebecque, A.; Massard, C.; Fuerea, A.; Ribrag, V.; Gazzah, A.; Armand, J. P.; Amellal, N.; Angevin, E.; Noel, N.; Boutros, C.; Mateus, C.; Robert, C.; Soria, J. C.; Marabelle, A.; Lambotte, O. Immune-related adverse events with immune checkpoint blockade: a comprehensive review. *Eur. J. Cancer.* **2016**, 54, 139–148.

(5) Miller, K. D.; Siegel, R. L.; Lin, C. C.; Mariotto, A. B.; Kramer, J. L.; Rowland, J. H.; Stein, K. D.; Alteri, R.; Jemal, A. Cancer treatment and survivorship statistics. *Cancer J. Clin.* **2016**, 66, 271–289.

(6) Pérez-Herrero, E.; Fernández-Medarde, A. Advanced targeted therapies in cancer: drug nanocarriers, the future of chemotherapy. *Eur. J. Pharm. Biopharm.* **2015**, 93, 52–79.

(7) Postow, M. A. Managing immune checkpoint-blocking antibody side effects. *Am. Soc. Clin. Oncol. Educ. Book.* **2015**, 35, 76–83.

(8) Therasse, P.; Arbuck, S. G.; Eisenhauer, E. A.; Wanders, J.; Kaplan, R. S.; Rubinstein. L.; Verweij, J.; Van, G. M.; van, O. A. T.; Christian, M. C.; Gwyther, S. G. New guidelines to evaluate the response to treatment in solid tumors. *J. Natl. Cancer Inst.* **2000**, 3, 205–216.

(9) Chen, Z.; Jiang, S.; Li, X.; Zhang, J.; Zhang, L. Efficacy and safety of anti-angiogenic drugs combined with erlotinib in the treatment of advanced non-small cell lung cancer: a meta-analysis of randomized clinical trials. *Ann. Palliat. Med.* **2021**, 10, 21037/apm-20-1621.

(10) Andrade, J. T.; Santos, F. R. S.; Lima, W. G.; Sousa, C. D. F.; Oliveira, L. S. F. M.; Rosy, I. M. A.; Ribeiro, R. I. M. A.; Gomes, A. J. P. S .; Araújo, M. G. F.; Villar, J. A. F. P.; Ferreira, J. M. S. Design, synthesis, biological activity and structure-activity relationship studies of chalcone derivatives as potential anti-Candida agents. *J. Antibiot.* **2018**, 71, 702–712.

(11) Lynch, T. J.; Bell, D.W.; Sordella, R.; Gurubhagavatula, S.; Okimoto, R. A.; Brannigan, B.W.; Harris, P. L.; Haserlat, S. M.; Supko, J. G.; Haluska, F. G.; Louis, D. N.; Christiani, D. C.; Settleman, J.; Haber, D. A. Activating mutations in the epidermal growth factor receptor underlying responsiveness of non-small-cell lung cancer to gefitinib. *New England J. Med.* **2004**, 350, 2129–2139.

(12) Paez, J. G.; Jänne, P. A.; Lee, J. C.; Tracy, S.; Greulich, H.; Gabriel, S.; Herman, P.; Kaye, F. J.; Lindeman, N.; Boggon, T. J.; Naoki, K.; Sasaki, H.; Fujii, Y.; Eck, M. J.; Sellers,W. R.; Johnson, B. E.; Meyerson, M. EGFR mutations in lung cancer: correlation with clinical response to gefitinib therapy. *Science* **2004**, 304, 1497–1500.

(13) Tsao, M. S.; Sakurada, A.; Cutz, J. C.; Zhu, C. Q.; Kamel-Reid, S.; Squire, J.; Lorimer, I.; Zhang, T.; Liu, N.; Daneshmand, M.; Marrano, P.; Santos, G. C.; Lagarde, A.; Richardson, F.; Seymour, L.; Whitehead, M.; Ding, K.; Pater, J.; Shepherd, F. A. Erlotinib in lung cancer-molecular and clinical predictors of outcome. *New England. J. Med.* **2006**, 353, 133–144.

(14) Zheng, Y. G.; Zhang, W. Q.; Meng, L.; Wu, X. Q.; Zhang, L.; An, L.; Li, C. L.; Gao, C. Y.; Xu, L.; Liu, Y. Design, synthesis and biological evaluation of 4-aniline quinazoline derivatives conjugated with hydrogen sulfide (H_2S) donors as potent EGFR inhibitors against L858R resistance mutation. *Eur. J. Med. Chem.* **2020**, 202, 112522–112532.

(15) Thorn, D. A.; An, X. F.; Zhang, Y.; Pigini, M.; Li, J. X. Characterization of the hypothermic effects of imidazoline I2 receptor agonists in rats. *Brit. J. Pharmacol.* **2012**, 166, 1936–1945.

(16) Nasr, M. N.; Gineinah, M. M. Pyrido 2,3-d pyrimidines and pyrimido 5´4´: 5,6 pyrido 2,3-d pyrimidines as new antiviral agents: synthesis and biological activity. *Arch. Pharm.* **2002**, 335, 289–295.

(17) Chandrika, P. M.; Yakaiah, T.; Rao, A. R. R.; Narsaiah, B.; Reddy, N. C.; Sridhar, V.; Rao, J. V. Synthesis of novel 4,6-disubstituted quinazoline derivatives, their anti-inflammatory and anti-cancer activity (cytotoxic) against U937 leukemia cell lines. *Eur. J. Med. Chem.* **2008**, 43, 846–852.

(18) Azzoli, C. G.; Ng, T. Commentary: preoperative gefitinib for stage II-III non-small cell lung cancer with EGFR mutation: a stich in time, or delay from stiches? *J. Thorac. Cardiovasc Surg.* **2021**, 161, 444–446.

(19) Sequist, L. V.; Waltman, B. A.; Dias-Santagata, D.; Digumarthy, S.; Turke, A. B.; Fidias, P.; Bergethon, K.; Shaw, A. T.; Gettinger, S.; Cosper, A. K.; Akhavanfard, S.; Heist, R. S.; Temel, J.; Christensen, J. G.; Wain, J. C.; Lynch, T. J.; Vernovsky, K.; Mark, E. J.; Lanuti, M.; Iafrate, A. J.; Mino-Kenudson, M.; Engelman, J. A. Genotypic and histological evolution of lung cancers acquiring resistance to EGFR inhibitors. *Sci. Transl. Med.* **2011**, 3, 75ra26.

(20) Li, D.; Ambrogio, L.; Shimamura, T.; Kubo, S.; Takahashi, M.; Chirieac, L. R.; Padera, R. F.; Shapiro, G. I.; Baum, A.; Himmelsbach, F.; Rettig, W. J.; Meyerson, M.; Solca, F.; Greulich, H.; Wong, K. K. BIBW2992, an irreversible EGFR/HER2 inhibitor highly effective in preclinical lung cancer models. *Oncogene* **2008**, 27, 4702–4711.

(21) Cross, D. A.; Ashton, S. E.; Ghiorghiu, S.; Eberlein, C.; Nebhan, C. A.; Spitzler, P. J.; Orme, J. P.; Finlay, M. R.; Ward, R. A.; Mellor, M. J.; Hughes, G.; Rahi, A.; Jacobs, V. N.; Red, B. M.; Ichihara, E.; Sun, J.; Jin, H.; Ballard, P.; Al-Kadhimi, K.; Rowlinson, R.; Klinowska, T.; Richmond, G. H.; Cantarini, M.; Kim, D. W.; Ranson, M. R.; Pao, W. AZD9291, an irreversible EGFR TKI, overcomes T790M-mediated resistance to EGFR inhibitors in lung cancer. *Cancer Dis.* **2014**, 4, 1046–1061.

(22) Miura, S.; Yamanaka, T.; Kato, T.; Ikeda, S.; Horinouchi, H.; Ichihara, E.; Kanazu, M.; Takiguchi,Y.; Tanaka, K.; Goto, Y.; Sata, M.; Hagiwara, K.; Okamoto, H.; Tanaka, H. Treatment rationale and design of a phase III study of afatinib or chemotherapy in patients with nonesmall-cell lung cancer harboring sensitizing uncommon epidermal growth factor receptor mutations. *Clin. Lung Cancer.* **2020**, 21, E592–E596.

(23) Liang, Q.; Wang, J.; Zhao, L.; Hou, J.; Hu, Y.; Shi, J. Recent advances of dual FGFR inhibitors as a novel therapy for cancer. *Eur. J. Med. Chem.* **2021**, 214, 113205–113205.